IEEE Access
Multidisciplinary | Rapid Review | Open Access Journal

Received December 9, 2019, accepted December 24, 2019, date of publication December 30, 2019,
date of current version January 10, 2020.

Digital Object Identifier 10.1109/ACCESS.2019.2962998

Synthesis of Linear and Planar Arrays via Sequential Convex Optimizations

ZHENGDONG QI[1,2], YECHAO BAI[1], AND XINGGAN ZHANG[1]
[1]School of Electronic Science and Engineering, Nanjing University, Nanjing 210023, China
[2]No.724 Research Institute of CSIC, Nanjing 210000, China

Corresponding author: Yechao Bai (ychbai@nju.edu.cn)

This work was supported by the National Natural Science Foundation of China under Grant 61571220 and Grant 61976113.

ABSTRACT In this paper, an iterative procedure for the synthesis of sparse arrays radiating focused beampattern is presented. The proposed approach provides a signifcant reduction in the complexity of the beam forming network, which is fulfilled by reducing the number of antenna elements in the array. An iterative scheme is used where the prescribed pattern response in the mainlobe is cast as a multi-convex problem at each step that the nonconvex lower bound constraint is relaxed while including a reweighted l_1-norm minimization based on the magnitudes of the elements. Thus, a sparse array with fewer elements (compared to other methods) and a better performance of beam pattern (e.g., narrower 3-dB beamwidth, lower maximum sidelobe level) is produced. The resulting sparse array is able to generate a steerable pencil beam, matching a given power mask and avoid to constraint the fitting of any a priori defined reference beam pattern. The practical array imperfections are also compensated in the optimization stage by using worst-case performance optimization technique. Examples concerning the design of linear and planar arrays show relevant savings of array elements with respect to conventional array techniques.

INDEX TERMS Array pattern synthesis, multi-convex programming, sequential convex optimization, sparse array.

I. INTRODUCTION

Reducing the number of elements in an antenna array provides several advantages over the conventional techniques, such as lower weight, cost, power consumption, and the minimization of the complexity of the Beam Forming Network (BFN). In digital beam forming array antenna systems, these advantages are reflected as a reduction in the computational load. The synthesis of reducing the number of elements is a nonconvex and highly nonlinear optimization problem, thus providing the global optimum solutions (i.e., good antenna selections) is very difficult, although good suboptimal solutions (rather than the globally optimal one) to the problem can be generally presented.

Generally the reduction of the number of array elements calls for the design of nonuniformly spaced antenna arrays. In such a framework, several different approaches have been proposed over the last few decades to synthesize such arrays. Among them one can mention stochastic optimization algorithms such as simulated annealing (SA) [1], [2], ant colony optimization (ACO) [3], genetic algorithm (GA) [4], particle swarm optimization (PSO) [5]. Unfortunately, these methods turn out being relatively time consuming, especially when dealing with the synthesis linear or planar arrays composed by a large number of antenna elements. Of course, in general, the achievement of the global optimum is not guaranteed due to the stochastic nature of the resolution algorithms. In addition, the hybrid method that combines the ACO and Least mean square algorithm is also utilized for the synthesis of thinned fractal array [6]. This work succeeds not only to steer the nulls in the directions of interferences and the mainlobe direction to desired angle, but also to maintain the similar radiation characteristics at diverse frequency bands with a reduced number of elements.

With the recent advances in convex optimization, few methods have lately shown a great significance and relevance on many applications in communications and signal processing. These hybrid synthesis algorithms, combining a stochastic optimization algorithm (SA or GA) to select the element locations and convex programming to obtain the element excitations, have thus been successfully implemented for solving multimodal and multidimensional

The associate editor coordinating the review of this manuscript and approving it for publication was Muhammad Ali Imran.

problems such as the sparse array synthesis [7] and [8]. In [9], a procedure to synthesize sparse arrays with antenna selected via convex optimization is presented. Despite its efficiency and success, the iterative method uses conjugate symmetric excitations and allows to synthesize only symmetric shaped beampatterns in order to keep the convexity of the problem. However, The symmetric weight constraint limits its result in real-valued patterns and thus lacks the degree of freedom (DOF) than that containing complex terms, and therefore, only symmetric power patterns are realizable, which preclude asymmetric sidelobe distribution. In practice, many applications require complex-valued array responses like scanned beams or shaped beam patterns. Especially, satisfactory solutions can be obtained thanks to the possibility of synthesizing asymmetric arrays (with more DOF) and to the simultaneous optimizations of the distribution of array elements excitations and positions.

In the framework of convex optimization, sparse-forcing methods have been extensively addressed by many researchers [9]–[13], and its implementation allows a strong reduction of the number of elements needed to achieve the design specifications. However, antenna synthesis is a slightly different problem compared to antenna measurements. It is to be noted that, while antenna measurements involve basically the solution of a finite-dimensional linear system, sparse array synthesis is a much more complex (and computationally expensive) case, since the space of unknowns (both the array coefficients and the positions of the elements are optimized) is, in principle, continuous. After reviewing the advantages and disadvantages of the existing methods, we present a new approach based on multi-convex programming for the synthesis of sparse arrays radiating focused beampattern. The provided solutions exhibit two key features which allow to maximize the radiation performance of beam pattern and minimize the weight and complexity of the BFN. First, differently from usual beam design methods for radar applications, the proposed design can achieve beampatterns characterized by arbitrary beamwidth (BW) and response ripple. By reformulating this non-convex lower bound constraints on the beampattern as an equivalent multi-convex optimization problem by adding two sets of auxiliary variables, a low complexity iterative algorithm which alternatingly adjusts the system variables and the auxiliary variables is proposed to solve the multi-convex optimization problem and find a stationary optimum. This facilitates the design of a mainlobe with controllable beamwidth and response ripple. In addition, arbitrary peak sidelobe level (PSL) can also be controlled. Unlike the mathematical programming methods [9], [13], [14] which are only applicable for symmetric purely-real arrangements, the proposed method based on multi-convex programming is feasible for complex syntheses such as asymmetric patterns(like, for instance, steerable beam patterns satisfying a prescribed power mask) or patterns with nulls towards the directions of clutter returns or jamming signals. Second, it shows and discusses different technique for the simplification of the array architecture. In order to utilize reweighted l_1-norm minimization inspired technique we have preliminarily to restrict the search space of the unknowns, in particular the element positions of the array, because of the fact that a reduction of the search space could result in an increase of the convergence rate. Additionally, only the array coefficients are optimized and the elements are fixed at predefined positions.Then, the computation time in our design is several (i.e. two or three) orders of magnitude smaller than previous methods involving Convex Programming (CP) procedure.

This results in a more efficient radiation pattern requiring fewer array elements that satisfies the same design specifications (concerning PSL and beamwidth) obtained by a non-sparse structure array. The proposed approach can be used to design nonuniformly spaced planar arrays with interelement spacings larger than halfwavelength, without the appearance of grating lobes in the focused beampattern.

Due to the practical array imperfections such as Mutual Coupling (MC) effects and other array calibration errors, the actual array manifold can be unknown and it can differ from the ideal presumed one. Thus, the synthesized pattern may degrade the radiation performance. For example, the traditional beampattern synthesis methods do not satisfy the provided specification on null design for practical fabricated arrays [15]. To compensate for undesirable effects in practice, robust beampattern constraints are derived in this paper based on the pre-calculated MC effects matrix and worst-case performance optimization technique. With use of the coupling matrix, the MC effects can be represented at an easy rate.

The communication is organized as follows. In Section II, the approach based on multi-convex programming for the synthesis of sparse arrays radiating focused beampattern is described. To show its efficiency, numerical comparisons with standard benchmark problems are showed in Section III. Conclusions are drawn in Section IV.

II. SYSTEM MODEL

Consider a linear array composed of $2N$ elements and assume the interelement spacing being Δd along the x-axis. For the sake of clarity, the problem is described for a one-dimensional pattern synthesis. The array factor $F(u)$ is given by

$$F(u) = \sum_{n=-N}^{N} a_n e^{jkn\Delta du} \tag{1}$$

wherein $j = \sqrt{-1}$, $k = 2\pi/\lambda_0$, λ_0 representing the wavelength in freespace, $u = sin\theta(\in [-1, 1])$. The weight vector $\boldsymbol{a} = [\boldsymbol{a}_{-N}, \ldots, \boldsymbol{a}_N]^T$ denoting the excitations for beam pattern. Defining the $2N$-dimensional array response vector by $\boldsymbol{w(u)} = [e^{jk(-N)du}, \ldots, e^{jkNdu}]$, (1) can be rewritten as $F(u) = \boldsymbol{w(u)a}$.

A. MULTI-CONVEX PROGRAMMING

The synthesis problem involves determining the weight vector a that maximize the radiation performance of beam pattern (e.g, narrow half-power beamwidth (HPBW) and low PSL).

Then, the final version of the optimization problem is

$$\sup_{(u)\in SB} \left| \left| \boldsymbol{w}(\boldsymbol{u})\boldsymbol{a} \right|^2 - d(u) \right| \leq \epsilon \tag{2a}$$

$$\left| \boldsymbol{w}(\boldsymbol{u})\boldsymbol{a} \right| \leq \rho(u) \quad (u) \in SL \tag{2b}$$

The power radiated by the array $|F(u)|^2$ is as close as possible to a desired shape $d(u)$, where $d(u) \in R^+$, in the main (shaped) beam region (denoted SB). The resulting array is able to minimize the maximum "distance" ϵ between the desired power pattern $d(u)$ and the field radiated by the array $|F(u)|^2$. The sidelobes, in the region (denoted SL), are kept below the envelop $\rho(u)$. Two nonoverlapping groups, SB and SL plotted in Fig.1, are then introduced. Let us notice that the mainlobe constraint in (2a) translates a maximization problem (discussed in [9], [13], [14]) into a minimization problem. As a crucial circumstance, the generic $\left| \boldsymbol{w}(\boldsymbol{u})\boldsymbol{a} \right| (u \in SL)$ is positive semidefinite quadratic form, so it can be shown constraint (2b) define a hypercylinder [16], and henceforth convex constraint, in the space of excitations. Although the constraint (2b) build a convex set and the objective function is convex, this is not the case of the shaped beam constraint (2a). To solve the problem, one can reformulate the above non-convex problem as equivalent multi-convex optimization problem with the addition of two auxiliary variables. Then, the optimal synthesis problem can be written as

$$\left| (\boldsymbol{w}\boldsymbol{a_l})^H \boldsymbol{w}\boldsymbol{a_r} - d \right| \leq \epsilon \quad with \quad \boldsymbol{a_l} = \boldsymbol{a_r} \tag{3a}$$

$$|\boldsymbol{w}\boldsymbol{a_r}| \leq \rho \tag{3b}$$

It yields the complex vector $\boldsymbol{w} = \boldsymbol{w}(\boldsymbol{u})$ and real positive numbers $d = d(u)$ and $\rho = \rho(u)$. $(\cdot)^H$ is the conjugate transpose, then, if one of the weight vectors $\boldsymbol{a_l}$ and $\boldsymbol{a_r}$ in (3) is fixed, the resulting one-variable cost function becomes convex, and the optimization problem (3a) gives rise to a CP problem. By fixing variables $\boldsymbol{a_r}$ for instance, the points $\boldsymbol{c} = \boldsymbol{a}_l^H \boldsymbol{w}^H \boldsymbol{w}$ are constraint, and the optimization problem can be stated as

$$|\boldsymbol{c}\boldsymbol{a_r} - d| \leq \epsilon \quad with \quad \boldsymbol{a_l} = \boldsymbol{a_r} \tag{4}$$

In the proposed design, the iterative algorithm need a guess (starting point) that is reasonably close to the optimal solution (the obtained element excitations fit the desired one in terms of PSL and mainlobe beamwidth), or else it is prone to be stuck at one of these local minima. This starting point should be chosen consistently with the problem(2). In this work, the definition of the point generating the patterns within the desired power constraints is given by means of an iterative projection method based on the Iterative Fourier technique (IFT).

Key characteristics of this Fourier technique algorithm are that the technique itself is highly robust, very simple, and very easy to implement in Matrix Laboratory (MATLAB), requiring only a few lines of code. The computational speed is very high, because the core calculations used in this technique are based on direct and inverse fast Fourier transforms. Such a technique is very well suited for the synthesis of large linear and planar arrays (See [17]–[24] for further details).

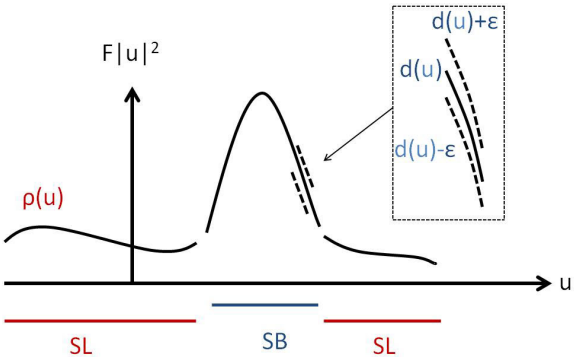

FIGURE 1. Schematic view of the focused beam synthesis problem.

The process to obtain a_l is an averaging operation to guarantee that asymptotically the difference between two variables vanishes. Since it is difficult to reach the optimum matching by manual adjustment, the smoothing algorithm [25] cannot ensure the equality among a_l and a_r as the number of iterations increases. In this paper, we propuse a heuristic way which amounts to update variable τ by minimizing the approximate constraint, the radiation pattern parameters δ and ρ are then updated and projected onto convex programming problem in the next iteration. Additionally, self-adjusting mechanism is introduced to determine the search direction, then the spatial datum point τ is substituted by its value determined in the previous step. τ for the $(k+1)$ th iteration turns out to be

$$\tau_{k+1} = \left(\boldsymbol{w}(\boldsymbol{u_0})(\boldsymbol{a_l})_k \right)^2 \tag{5}$$

where u_0 is the observation direction.

The maximum ripple $A_{ML}(> 0)$ of main beam is defined as

$$-A_{ML} \leq 20log10\left((\sqrt{d_k} - \delta_{k+1})/\sqrt{\tau_{k+1}} \right) \leq 0 \tag{6}$$

$$or \quad 0 \leq 20log10\left((\sqrt{d_k} + \delta_{k+1})/\sqrt{\tau_{k+1}} \right) \leq A_{ML} \tag{7}$$

where $\delta_{k+1} > 0$ indicate the distance between two successive solutions d_{k+1} and d_k. According to the sandwich theorem, (7) is selected. As variation of τ between two successive iterations becomes small with the convergence of the algorithm, we have that $\tau_k = \tau_{k+1}$. Then, the nonconvex constraint in the denominator is relaxed by replacing the update τ_{k+1} with τ_k, the maximum value of δ is given by

$$\delta_{k+1} \approx \sqrt{d_k} - \sqrt{\tau_k} 10^{\frac{-A_{ML}}{20}} \tag{8}$$

The shaped beam constraint that can be formulated as follows

$$\epsilon_{k+1} = |d_{k+1} - d_k| \approx 2(d_k - \sqrt{d_k}\sqrt{\tau_k} 10^{\frac{-A_{ML}}{20}}) \tag{9}$$

Sidelobe constraint UB, is defined according to the envelop ρ in (2b), given by

$$UB_{k+1} = \sqrt{(\tau_k)}(10^{(\frac{\rho}{20})}) \tag{10}$$

Notablely, the robustness of the proposed approach is improved since there is no parameter to be tuned.

B. THE SYNTHESIS OF SPARSE ARRAY

In this paper, the aim of the proposed design is to synthesise a sparse array so as to match beampattern with minimum number of elements, the synthesis problem can be written as

$$\min_{\boldsymbol{a}} \|\boldsymbol{a}\|_0 \quad under(2) \tag{11}$$

The l_0-norm minimization problem is an NP-hard combinatorial optimization problem and generally impossible to solve, as its globally optimal solution usually requires an intractable combinatorial search, even for a modest-sized array. In order to circumvent the intractable problem, we relax (11) by replacing the l_0-norm with the following l_1-norm

$$\min_{\boldsymbol{a}} \|\boldsymbol{a}\|_1 \quad under(2) \tag{12}$$

Note that the l_1-norm is the closest convex function to l_0-norm. An algorithm involves performing a sequence of reweighted convex l_1 minimization problems has been developed in [9]–[13], [26], [27]. By relaxing $\min_{\boldsymbol{a}} \|\boldsymbol{a}\|_0$ to weighted l_1 minimization problem, the vector a is minimized at $(k+1)$th iteration as

$$\min_{\boldsymbol{a}} \sum_{n=-N}^{N} \frac{|(\boldsymbol{a_n})_{k+1}|}{|(\boldsymbol{a_n})_k| + \mu} \quad with \quad \mu > 0 \tag{13}$$

The threshold μ, whose value is set slightly larger than the zero, is used to provide stability when $|(\boldsymbol{a_n})_k| = 0$. Notably, in the first iteration ($k = 1$), a unweighted l_1-norm of (12) is solved.

C. ROBUSTNESS ISSUES

In order to include effect of mutual coupling among antenna arrays for array application of beampattern synthesis, we insert a mutual coupling matrix to modify array steering vector (ASV). The mutual coupling matrix is transformed from mutual impedance matrix which can be obtained by using many mutual coupling compensation methods [9] and [15]. By using worst-case optimization technique, the error between the actual steering vector $\widetilde{\boldsymbol{w}}(\boldsymbol{u})$ and the ideal presumed one $\boldsymbol{w}(\boldsymbol{u})$ are compensated by coupling $\boldsymbol{C}$. Assume that the actual steering vector $\widetilde{\boldsymbol{w}}(\boldsymbol{u}) = \boldsymbol{C}\boldsymbol{w}(\boldsymbol{u})$ is

$$\widetilde{\boldsymbol{w}}(\boldsymbol{u}) = \boldsymbol{w}(\boldsymbol{u}) + \boldsymbol{e}(\boldsymbol{u}) \tag{14}$$

where $\boldsymbol{e}(\boldsymbol{u})$ is the complex error, its norm is limited by $\|\boldsymbol{e}(\boldsymbol{u})\|_2 \le \eta(u) = \eta$ (for simplicity), $\|.\|_2$ is the matrix two-norm. The previous proposed sidelobe constraint is rewritten as $\max|\widetilde{\boldsymbol{w}}(\boldsymbol{u})a| \le UB$. Applying the triangle and Cauchy-Schwarz inequalities along with the inequality $\|\boldsymbol{e}(\boldsymbol{u})\|_2 \le \eta$, we have that

$$\begin{aligned} |\widetilde{\boldsymbol{w}}(\boldsymbol{u})\boldsymbol{a}| &= |\boldsymbol{w}(\boldsymbol{u})\boldsymbol{a} + \boldsymbol{e}(\boldsymbol{u})\boldsymbol{a}| \\ &\le |\boldsymbol{w}(\boldsymbol{u})\boldsymbol{a}| + |\boldsymbol{e}(\boldsymbol{u})\boldsymbol{a}| \\ &\le |\boldsymbol{w}(\boldsymbol{u})\boldsymbol{a}| + \eta \|\boldsymbol{a}\|_2 \le UB \end{aligned} \tag{15}$$

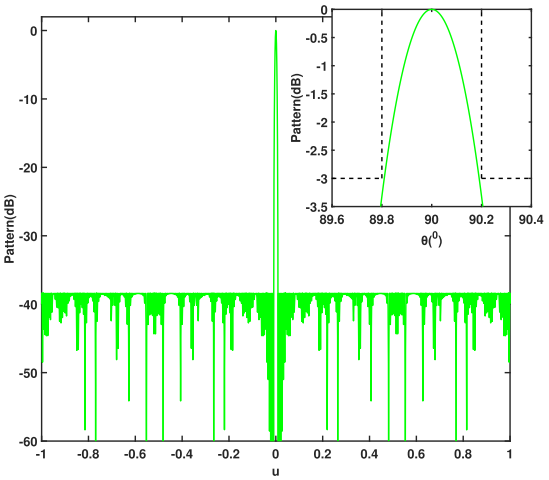

FIGURE 2. The pattern synthesis with 177 elements, the PSL is −38.32dB.

It can be shown that the constraints (15) define convex sets in the space of the unknowns. Consequently, the synthesis problem is formulated as the determination of the weight vector a such that

$$\begin{aligned} &\min_{\boldsymbol{a_{k+1}}} \sum_{i=-N}^{N} \frac{|(\boldsymbol{a_i})_{k+1}|}{|(a_i)_k| + \mu} \quad with \quad \mu > 0 \\ &|\boldsymbol{c}\boldsymbol{a_r} - d| \le \epsilon \quad with \quad \boldsymbol{a_l} = \boldsymbol{a_r} \\ &|\boldsymbol{w}\boldsymbol{a_r}| + \eta \|\boldsymbol{a_r}\|_2 \le UB \end{aligned} \tag{16}$$

Note that, different from the methods proposed in [9], [13], [14] which allow to synthesize only conjugate-symmetric excitation assumption in order to keep the problem convex, the proposed method can be extended to the synthesis of scanned beams or shaped beams with complex-valued responses. Algorithm 1 shows the sketch of the approach.

Algorithm 1 The Design of Linear and Planar Sparse Arrays Radiating Focused Beam Patterns

procedure SHAPEDBEAM
$a, a \longleftarrow$results based on the IFT method ▷Initialization
while i<I(The maximum allowed number of iterations) or $|\|\boldsymbol{a_l}\|_1 - \|\boldsymbol{a_r}\|_1| > 10^{-7}$ **do**
$\boldsymbol{c} = \boldsymbol{a_l}^H \boldsymbol{w}^H \boldsymbol{w}$ Solve (16) to get $\boldsymbol{a_l}$
$\boldsymbol{a_r} \longleftarrow \boldsymbol{a_l}$
end while
return $\boldsymbol{a}$
end procedure

III. REFERENCE EXAMPLES

To assess capabilities and performances of the proposed synthesis approach, some benchmark problems usually found in the literature concerning the synthesis of nonuniformly spaced linear and planar arrays are considered in the following.

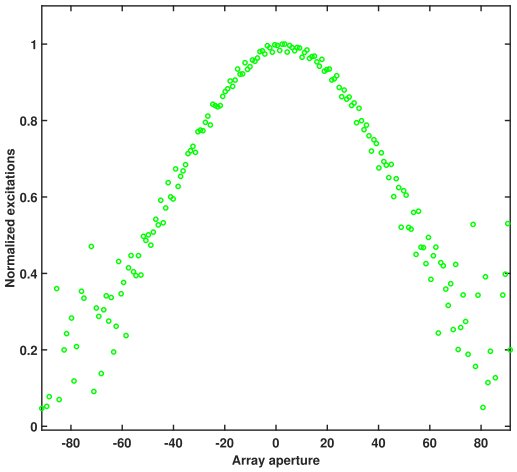

FIGURE 3. Synthesized excitation amplitudes for the focused beampattern. Design parameters: Ne=177, Aperture size=182.744λ.

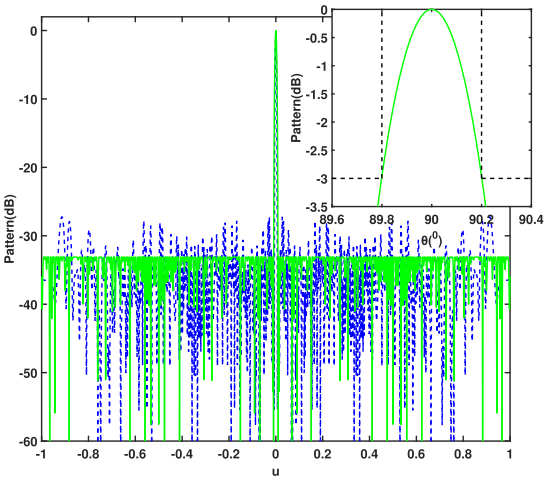

FIGURE 4. The pattern synthesis with 160 elements, the PSL is −33.05dB. Solid line and the dashed line represent the corrected pattern and the damaged pattern, respectively. The figure shows that the *BW* of the corrected pattern is the same as the *BW* of the original one.

A. MINIMIZE THE PSL FOR LINEAR ARRAY

As the first numerical simulation to validate the proposed approach, a sparse linear array whose element positions and excitations are optimized by hybrid method (which involves a nonuniform Fourier transform and a SA procedure together, NUFFT-SA) in [28], Fig. 3, is considered. The optimized sparse array has a −35.12 dB PSL and 0.4° HPBW in a 249.46λ aperture. In this case, an initial array, with a maximum aperture of 249.46λ, composed of 259 elements is considered as a starting point to synthesize the desired focused beampattern. The constraints (16) are applied with $\mu = 0.45$ and $A_{ML} = 0.01$dB. As can be seen in [28], our approach can achieve a 3.2dB lower PSL than that provided by competing design ($PSL_{Multi-convex} = -38.33$dB vs. $PSL_{NUFFT-SA} = -35.12$dB). Fig. 2 shows the synthesized pattern by using the approach herein proposed with Ne=177 elements, the amplitude and position distributions are nonuniform while all excitation phases are zeros. Compared with the 473 nonuniform (amplitude and phase) elements synthesized by the competing method, our method reduces the required number of antennas by 62.58%. Furthermore, the size of spatial aperture in our design is 182.744λ, which is decreased by roughly 26.74% compared to that in [28]. The minimum, average, and maximum spacing between adjacent elements turned out being equal to 0.9669λ, 1.0383λ and 2.9007λ, respectively, thus alleviating the mutual coupling amongst the elements. The amplitude only control used in the work reduces the complexity of the BFN because it needs only the attenuators and not phase shifters which is required in phase control approach. Moreover, the achieved antenna layout and excitations are determined just after 5 iterations, the CPU time required to complete the iterative loop is equal to 60 seconds. In the first four iterations, the desired power pattern mask on the mainlobes and sidelobes was discretized by using 644 samples uniformly-spaced in the normalized angular domain u, in the last iteration (k = 5), the desired pattern was synthesized giving a total of 3316 points.

If several elements of the array are damaged, the PSL may increase dramatically [29] and [30]. One may want to optimize the excitations (amplitude only control) of the remaining elements to control the radiation performance. Seventeen failure elements are randomly chosen (i.e., the 1th, 2th, 4th, 7th, 10th, 12th, 22th, 26th, 30th, 51th, 54th, 126th, 150th, 151th, 153th, 167th, and 170th elements, which is 10% of the total number of active elements), and the proposed approach is carried out to recalculate the amplitudes to reduce the PSL and keep HPBW to be equal to the original(undamaged) one. As shown in Fig. 4, the PSL of the corrected pattern is −32.76dB, which is 5.57 dB higher than the original one but 5.53dB lower than the damaged pattern (with original amplitudes and 17 elements failures). The corrected pattern has the same HPBW as the original pattern (Fig.2). Thanks to the efficiency of CVX slover, the proposed approach can correct the array pattern, which are degraded by element failures, in almost real time (i.e., 14.5s). All the simulations have been obtained for a PC equipped with an Intel(R) Core(TM) i5-6500T (3.4 GHz) provided with 12 GB of RAM memory and running 64-bit Windows 10. The software coding of the proposed method have been implemented under the MATLAB programming platform R2014a and convex problem solver (CVX [31]).

Next, larger linear arrays are applied to compare the proposed approach with a NUFFT method, stochastic optimization algorithm and convex optimization approach [32]. The initial array size are selected as 180λ, 210λ, 240λ, 270λ, 300 λ and 330 λ, and their corresponding initial element number is 191, 221, 251, 281, 311 and 341, respectively. For each linear array, the element positions are fixed at predefined positions with the minimum spacing between adjacent elements greater than 0.94λ. The desired pattern is to minimize the PSL with a prescribed mainlobe area [−0.36° 0.36°]. Table 1 gives the simulation results with different

TABLE 1. The simulation results in the CVX, the PSO, the NUFFT and the Proposed design with difierent initial elements.

Aperture size[λ]	Number of Element	Peak Side Lobe Level (dB)			Proposed Multi-convex approach		
		CVX[28]	PSO[28]	NUFFT[28]	Size[λ]	PSL(dB)	Element
180	326	-25.1	-18.1	-24.6	144.95	-25.19	75
210	401	-30.2	-22.5	-29.9	147.95	-30.27	90
240	476	-35.6	-25.4	-35.1	198.72	-35.64	109
270	551	Failed	-29.3	-40.2	208.29	-40.24	118
300	626	Failed	-34.9	-45.5	272.90	-45.60	132
330	701	Failed	-35.5	-50.9	309.62	-51.11	149

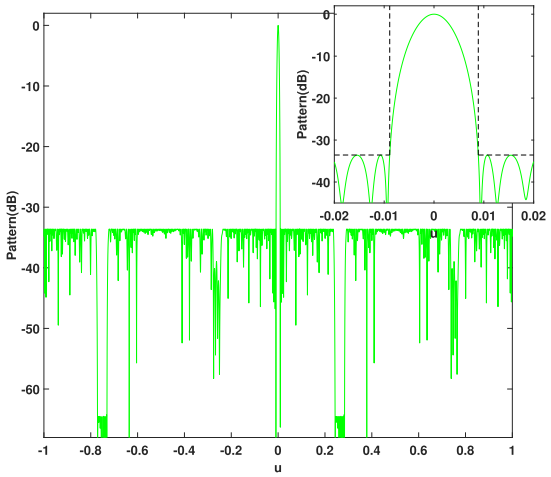

FIGURE 5. The pattern synthesis with 170 elements, the PSL is −33.5645dB and and all the null regions are smaller than −64.23dB.

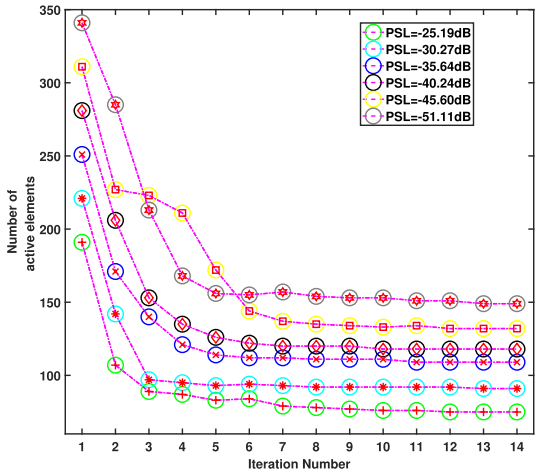

FIGURE 6. Convergence of the number of active elements versus the number of iterations.

geometries and target patterns obtained by the proposed approach and shows the comparisons with other optimisation methods. As far as the array layouts are concerned, it is worth noticing that, the reduction in the aperture by 6.2% $\sim$ 29.6% and the reduction in the number of elements by 77.0% $\sim$ 78.9%, both obtained by the multi-convex approach, are not accompanied by a worsening of the *PSL* and *BP* (see Table 1). The number of iterations is typically very small (less than 13 for all the synthesis problems, as evidenced in the Fig. 6), so that the additional computational cost is not prohibitive. This example illustrates the reliability and efficiency of the proposed approach for the optimization of electrically large linear arrays.

In this case, the null control is added into design requirements for a sparse linear array. In order to investigate the robustness of the solutions presented in the presence of MC effects and other array calibration errors, robust constraint for the sidelobe region is used with the proposed method (16) where $\eta = 0.017$. The number of required elements is minimized by minimizing the cardinality of the current distribution through its reweighted l_1-norm. A 333-elements array is initialized from the proposed design and the array aperture is 327.3λ. The optimization goal is to minimize the PSL with a prescribed mainlobe area as [−0.0089,0.0089]. In addition, a depression of about 30 dB below the sidelobe level has been imposed for the angular direction having [−76.7°, −74.4°] and [14.1°, 15.9°]. Fig.5 shows the PSL is equal to −33.56 dB, that is about 1.3 dB lower than that obtained with the method in [28], and the null regions are smaller than −64.23 dB (rather than −52 dB reported in [28]) with the 170 elements. Obviously, the number of array elements is reduced more than 31.2% through the proposed method. Finally, the aperture size in our design is slightly smaller than 349.46λ [28], which is equal to 326.31λ. As a matter of fact, the maximally sparse solution presents not only a lower PSL value but also a considerably narrower *BW* (i.e., $BW_{Multi-Convex} = 0.0178$ versus $BW_{NUFFT-SA} = 0.0720$). Such a result further confirms the effectiveness of the proposed design in dealing with the nonconvex part of the problem at hand, thus allowing the synthesis of focused beampatterns with better characteristics.

B. MINIMIZE THE PSL FOR PLANAR ARRAY

As first comparison, we will consider the specifications discussed in [33], where 49 elements were required to synthesize a pencil with a 6-dB main beam width of $\sin(\theta_{bw}) = 0.237$ a side lobe level of −17.6dB. The similar radiation performance, with multi-convex programming formulation with 35 elements only (see Fig. 7) within an array aperture of $25\lambda^2$. The element locations and the associated normalized

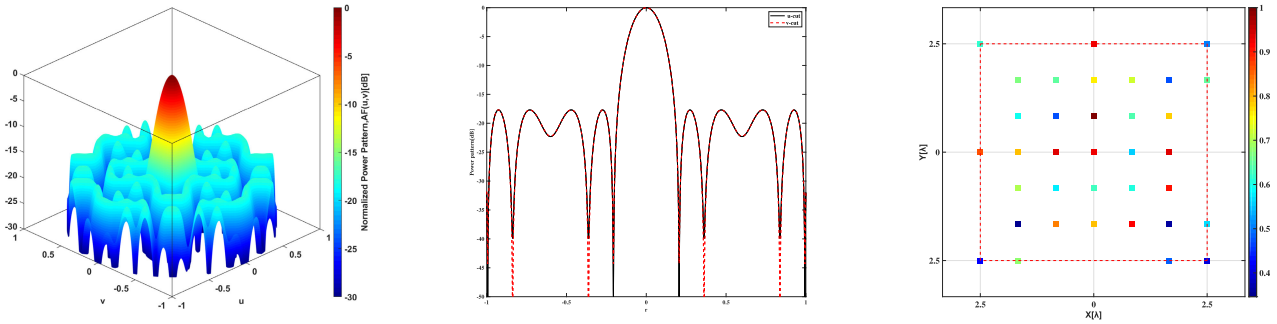

(a) (b) (c)

FIGURE 7. Sparse planar array synthesis results: (a) 3D view of the far field pattern with (b) *u* and *v* cutting planes and (c) optimized layout of the 35 element array.

TABLE 2. Coordinates and normalized weights: Focused beam.

No.	(x[λ],y[λ])	w(x,y)	12	(x[λ],y[λ])	w(x,y)	No.	(x[λ],y[λ])	w(x,y)
1	(-2.50 -2.50)	0.4035	13	(-0.83, 0)	0.6253	25	(0.83, 0.83)	0.4695
2	(-2.50 -1.67)	0.4807	14	(-0.83, 0.83)	0.5733	26	(0.83, 1.67)	0.5958
3	(-2.50 1.67)	0.6745	15	(-0.83, 1.67)	0.7030	27	(1.67, -2.5)	0.6449
4	(-2.50 2.50)	0.4199	16	(0, -1.67)	0.9378	28	(1.67, -1.6)	0.4709
5	(-1.67, -2.50)	0.5662	17	(0, -0.83)	0.5601	29	(1.67, -0.83)	0.7165
6	(-1.67, -1.67)	0.3582	18	(0, 0)	0.9200	30	(1.67, 0)	0.7566
7	(-1.67, -0.83)	0.9099	19	(0, 0.83)	0.9366	31	(1.67, 0.83)	0.6498
8	(-1.67, 0)	0.7951	20	(0, 1.67)	0.7942	32	(1.67, 1.67)	0.6724
9	(-1.67, 0.83)	0.8358	21	(0, 2.5)	0.8662	33	(2.5, -2.5)	0.5039
10	(-1.67, 1.67)	0.3462	22	(0.83, -1.67)	0.7795	34	(2.5, 0)	0.9188
11	(-0.83, -1.67)	0.9038	23	(0.83, -0.83)	0.6415	35	(2.5, 2.5)	0.6142
12	(-0.83, -0.83)	0.6056	24	(0.83, 0)	1.0000			

excitations, whose dynamic range ratio ($|w_{max}|\,/\,|w_{min}|$, DRR) is 2.89, are reported in Table 2. The achieved layout exhibits a maximum directivity $D_{MAX} = 18.97$dB, the minimum inter-element distances is 0.83λ. It is worth underlining that the case of [33] has been considered, with small variations of the PSL and of the beamwidth, also in other papers. The proposed method is computationally efficient (e.g., the CPU time is just 1.3 min for the synthesis of a 49-element uniform array, including the process of finding the minimum element number). It is stressed that the PSL of the sparse array turned out to be about 0.3 dB lower than that of the CS-based weighted-norm one [27], which however saves almost 15% (1-35/41) of the elements, and requires less CPU time. In [10] an array of 35 elements is achieved in six hours; instead, in [11] a layout with 33 radiating elements is achieved in about 100 minutes. Table 3 provides the comparison results of these four approaches. As for the computational costs, the poposed design provides about two orders of magnitude faster computing speed compared with Inflating-Deflating Exploration Algorithm (IDEA), and three orders of magnitude that compared with the multi-level branch-and-bound (B&B). As far as the number of elements are concerned, it should be noticed that the initial array aperture in [11] is increased form $25\lambda^2$ to $32.2301\lambda^2$ ($5.952\lambda \times 5.415\lambda$). Such an additional DOF for the solution space can be exploited to improve the array performance of the competing method.

The second example is aimed at demonstrating the validity of the proposed approach to the design of large planar array with circular boundaries (i.e., a non-rectangular shape). A concentric circular array is considered as in [28]. There are 20 rings and a single element at the center. The radius of the nth ring is $r_n = 0.6n\lambda$. In the nth ring, there are $[2\pi n]$ elements uniformly distributed. That is a nonuniform array and the total element number is 1310. The optimization goal is to minimize the PSL with the mainlobe region restricted to $\{(u)|\sqrt{u^2+v^2} \le 0.074\}$. The result from the NUFFT-SA [28] has a PSL of -37.05 dB with 718 elements.

In contrast to [28], a planar array with $2M \times 2N = 28 \times 28$ elements has been taken into account with an inter-element distance along the x and y axis equal to $d_x = d_y = 0.889$. Accordingly, the circular aperture has been generated by imposing to zero the excitations of the elements outside a circular contour of radius $R_s = 12.1\lambda$, as in Fig.8. Fig.9 gives the pseudocontour plot of one simulation result. The u and v cut patterns are in Fig.10. The corresponding amplitude

TABLE 3. The comparison of sparse array results of the four approaches with earlier published theoretical results involves mainly the antenna radiation characteristics.

Competing Algorithm	Matrix pencil method [33]	CS-based weighted-norm approach[27]	Multi-level branch-and-bound (B&B) [10]	Inflating-Deflating Exploration Algorithm[11]	Proposed multi-Convex Programming
Elements	49	41	35	33	35
BW= $\sin(\theta_{bw})$[rad]	0.237	0.240	0.240	0.237	0.2382
PSL[dB]	-17.6	-17.3	-17.5	-17.6	-17.637
Aperture size [λ^2]	22.29	< 25	21.11	22.7881	25
Computation time[min.]	/	4	3600	100	1.3

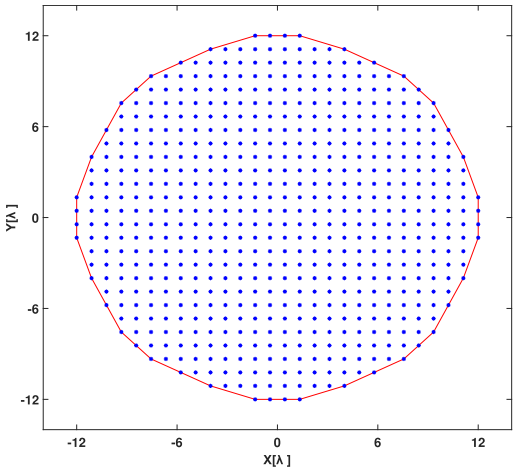

FIGURE 8. A planar array with $2M \times 2M = 28 \times 28$ elements has been taken into account with an inter-element distance along the x and y axis equal to $d_x = d_y = 0.8889$. The initial (blue marked) elements are the ones selected by the circle of radius 12.1λ.The area bounded by the convex hull is $443.26\lambda^2$.

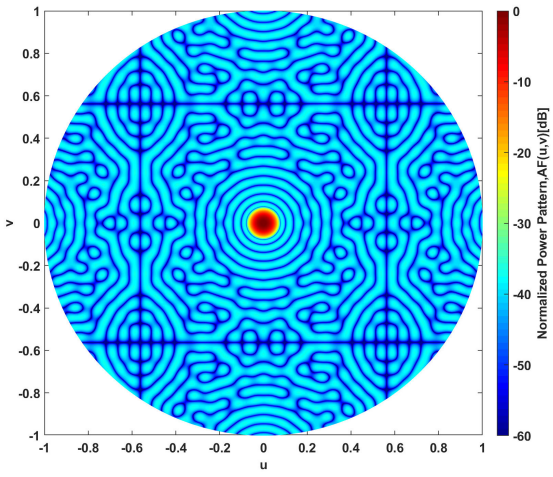

FIGURE 9. Pesudocontour plot of the planar array, which is restricted to be smaller than −37.12 dB.

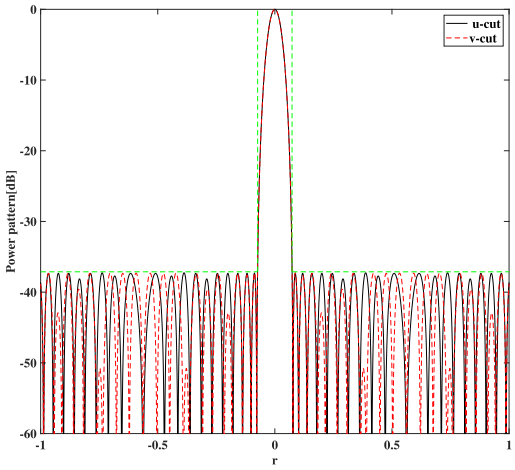

FIGURE 10. Beampattern cuts at $u = 0$ and $v = 0$ of the synthesized pattern.

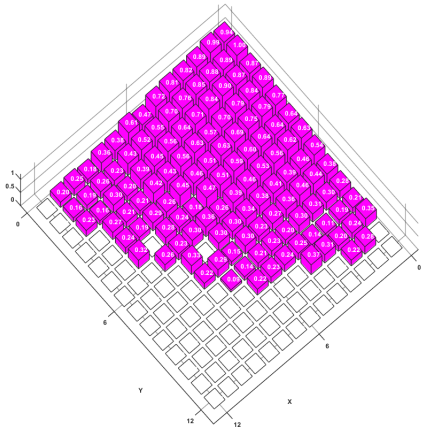

FIGURE 11. Resulting steerable array layout relative to the synthesis of focused beam power pattern. Active radiating elements Ne=512. The area bounded by the convex hull is $397.43\lambda^2$.

excitations are reported in Fig.11. Note that only one quadrant of the whole array is plotted by virtue of the quadrantal symmetry of the antenna. As it can be observed, the 512 elements layout achieving a side lobe level lower than −37.12dB for $\{(u)|\sqrt{u^2+v^2} \leq 0.0735\}$. Only 87.7% antenna array is used in this case. We observe that the proposed design has better radiation performance (e.g., narrower 3-dB beamwidth, lower maximum sidelobe level) and the number of array elements is decreased by 28.7% compared to that in [28]. In the proposed design, the radiating elements are disposed in a centrosymmetric fashion with respect to the array center. The broadside

TABLE 4. Input parameters: Array edge, Initial elements.

Initial size[λ^2]	Initial elements	BW	PSL [dB]	Size[λ^2]	N_e
443.26	584	0.0734993	-37.1210	397.43	512
			-38.1430	410.07	548
			-39.1531	429.04	564
			-39.9164	443.26	584
561.56	680	0.0734993	-37.2255	405.52	488
			-38.1961	412.38	504
			-39.1500	436.39	532
			-40.1758	438.10	536
		0.0729771	-42.0922	499.83	600

focused (pencil) beam pattern is generated by imposing a quadrantal symmetry of the excitation amplitudes: the beam is generated when all quadrants are excited with the same phase. Notably, the provided solutions exhibit a key feature which allows the minimization of the weight and complexity of the BFN. Finally, the size of spatial aperture in our design is $397.4\lambda^2$, which is decreased by 12.5% compared to that in [28]. The minimum spacing between adjacent elements is constrained between the limits $0.889 \leq$dx and $0.889 \leq$dy, this suggests the MC effects among antenna array are very small that it can be neglected.

Then, for different PSLs, the synthesis problem (16) is solved in order to determine the minimum number of the required active antenna elements. Specifically, the considered array size and the BW together with the relative optimum PSL are reported in Table 4. Interestingly, as it can be seen from Table 4, the minimum number of required active elements decreases as the array size and initial number of array elements increases, showing that there are more DOF for the optimization/sparsification problem (for the considered aperture sizes).

Moreover, it should be noted that the number of actual unknowns is equal to just a quarter of the overall number of excitations. Here we must point out that although Algorithm 1 also uses the reweighted l_1-norm scheme, the introduced pair-sparsity in it for symmetric excitation costs some freedom degree of weight vector. As a result, the obtained result is less sparse than that of array with asymmetrical aperture.

To explore the ability of Algorithm 1 to synthesize the beampattern of asymmetric planar array, we simulate an asymmetric antenna array (see initial aperture distribution in Fig.12). Here the same beampattern synthesis configuration ($BW = 0.0734993$, $PSL = -37.2348$) as that of the above example is used. In this case, the weight coefficients are restricted to take on only real values here. Then, thanks to the potentialities of convex solvers, the possibility of designing asymmetric planar arrays, i.e., with a larger number of DOF, is fully exploited. Fig.12 plots the corresponding beampattern slices of the u and v direction generated by Algorithm 1, which shows that the generated beampattern meets the

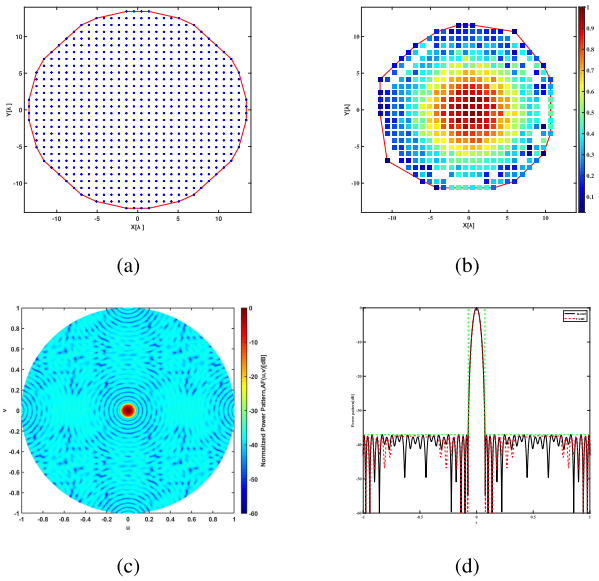

FIGURE 12. (a) A planar array with $2M \times 2M = 30 \times 30$ elements, $d_x = d_y = 0.9259$. The initial elements are the ones selected by the circle of radius 13.5 λ. (b) Resulting array layout relative to the synthesis of focused beam power pattern.The area bounded by the convex hull is $408.1\lambda^2$. Active radiating elements Ne=462. (c) Pesudocontour plot of the planar array with restriction of mainlobe width. (d) Beampattern cuts at u = 0 and v = 0 of the synthesized pattern shown in (c).

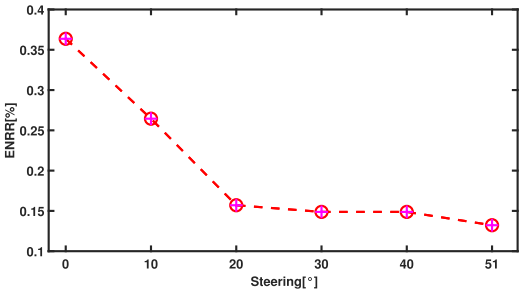

FIGURE 13. Number of active elements N_e Vs Steering angles for BWs and PSLs of Table 4.

mainlobe and sidelobe constraints. In Fig.12, we show the positions of 462 selected elements and the complete asymmetric array.

From these considerations, we can conclude that for asymmetric planar array, Algorithm 1 leads to more zero excitation antennas than symmetrical aperture case due to the freedom degree increase resulted from a proper relaxation of the pair sparsity constraints on weight elements. Furthermore, the obtained results clearly indicate that the proposed approach can be of interest when the number of DOF of the high-dimension synthesis at hand is very large and computationally unfeasible for stochastic optimization methods. Clearly, this represents a major advantage for larger arrays.

Basically speaking, such stochastic optimization methodology [28] is prone to stuck in local optimum and cannot be easily applied to planar arrays composed by a large number of elements owing to the convergence issues and the arising computational burden. Then, the achievement of provably

optimal solutions is not guaranteed due to stochastic nature of the resolution algorithms. We should point out that the competing methods [28] and [32] require choosing appropriate parameter values to obtain a suboptimal solution. One cannot choose the state optimal control parameters for the first time, and several attempts may be required. Thus, the computational load will be drastically increased. However, there is no parameter to be tuned for CVX slover (fixed parameter μ). Moreover, since software package CVX (SDPT3 and SEDUMI as its main optimization solvers) allow, nowadays, to handle large array synthesis problem that involve millions of variables, the excellent performances in terms of computational efficiency and the best achievable array and radiation performance obtained in this work (or even larger problems) demonstrate the proposed approach more attractive than NUFFT and global optimization technique which, as previously observed, do not assure convergence (to optimal solutions) and can become prohibitive in the case of large planar arrays.

C. MAXIMALLY SPARSE AND STEERABLE ARRAYS

Let us now evaluate the performance of the proposed approach in the design where a given (steering) angular position is assigned for the given mask, which is of great interest in the case of Active Electronically Scanned Array (AESA) systems. More in detail, *SB* in (2b) is the region out of the assigned mainbeam (whose extension are kept below the PSL) such that $u^2 + v^2 \leq [1 + sin(\theta_M)]^2$, where θ_M is the angle with respect to the broadside direction of the array, so to extend the constraint outside the visible space in the (u, v) region and automatically avoide possible grating lobe (when making linear steering).

In this design an increased number of array elements, with respect to the broadside 3-D pattern, is expected. This experiment aims to assess how the saving in the number of antenna elements vary with respect to the amplitudes of the steering range. In each synthesis problem, for a fair comparison, the desired power mask to fulfill is optimal in the Chebyshev pattern (see Table 3 in [11], $Ne = 121$, N_e is the number of active elements, $PSL = -24.3877$dB, $BW = 25.3326°$) for the prefixed element positions. More in detail, the numerical assessment in performed by fixing, as input parameters, the initial number of array elements and the associated maximum sidelobe level for a given beamwidth. Then, for different values of the steering angle, the search for the solution is carried out in order to select the minimum number of active elements.

In this example, a planar array with $M \times N = 11 \times 11$ elements has been taken into account with an inter-element distance along the and axis equal to $d_x = d_y = 0.5$. The proposed resolution method has been applied to perform the optimization of the array design, for different steering directions whose extension vary in the range of 0° to 51°. A set of numerical results are plotted in Fig. 13, recalling the definition of Elements Number Reduction Ratio (ENRR) [11] as ENRR $= 1 - N_e/(M \times N)$, which represents the trend of

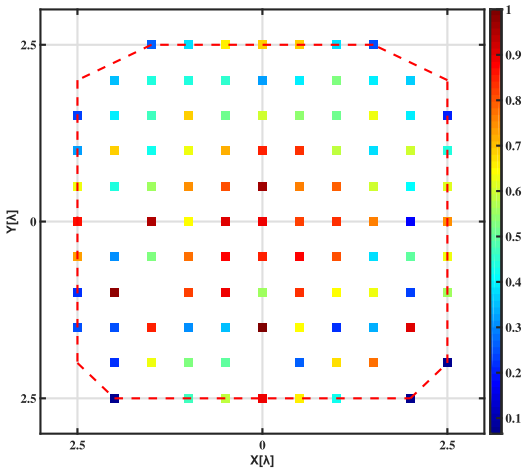

FIGURE 14. Resulting steerable array layout relative to the synthesis of focused beampattern. Edge size 5λ. Discretization grid: dx = dy = 0.5λ. Steering range $\theta_m = 51°$. The dashed curve represents the convex hull. Active radiating elements Ne=105.

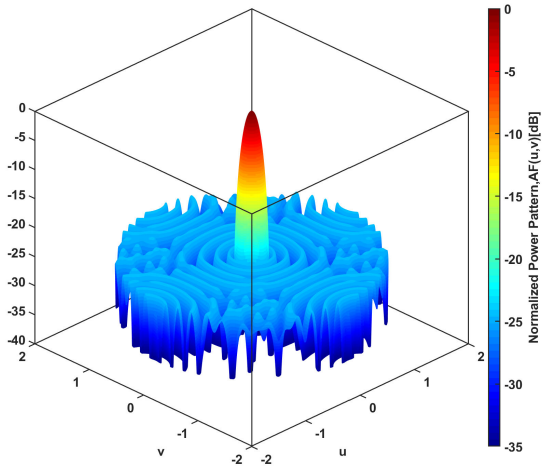

FIGURE 15. 3D power pattern radiated by the 5λ steerable array (Fig. 14) pointing at broadside. Ne=105 active radiating elements. BW = 25.3°, PSL = −24.3dB.

TABLE 5. ENRR Vs Steering angles for BWs and PSLs.

Steering angle	Size [λ^2]	BW[deg]	PSL [dB]	N_e
0°	23.75	25.3500	-24.3459	77
10°	23.87	25.3377	-24.3663	89
20°	22.50	25.3361	-24.3186	102
30°	23.00	25.3361	-24.3111	103
40°	22.75	25.3361	-24.3021	103
51°	23.625	25.3056	-24.3430	105

the reduction in the number of array elements with respect to the steering intervals.

Fig.13 clearly depicts how the converge ENRR toward the final solution as the steering angle reaches the maximum one. The sparse array is able to radiate a power pattern that satisfies the radiation characteristics in Table 5, in the considered steering direction that extends up to $\theta_M = 51°$ for each value

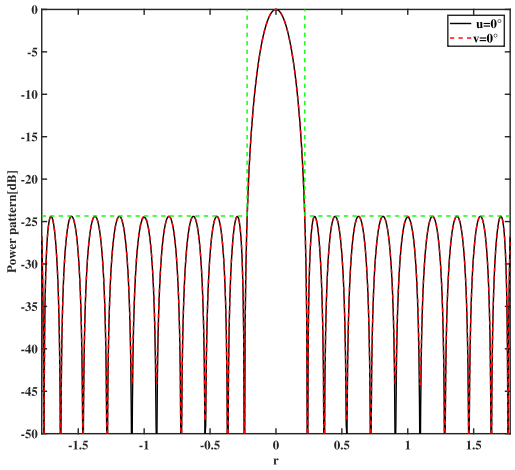

FIGURE 16. *u*-cut and *v*-cut of the synthesized pattern radiated by the array in Fig. 14 with Ne=105 active radiating elements.

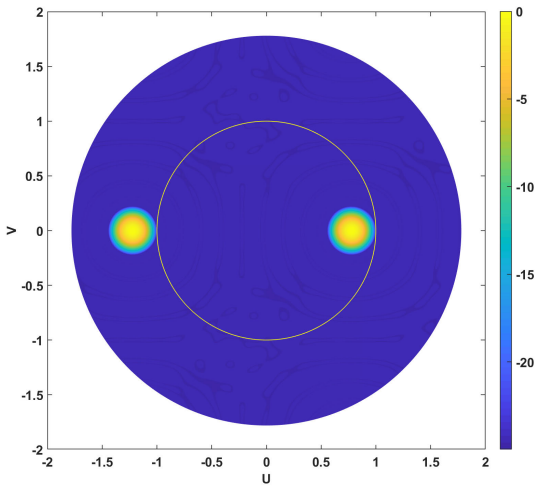

FIGURE 17. 2D power pattern radiated by the 5λ steerable array (Fig. 14) pointing at $(\theta, \phi) = (51°, 0°)$. BW = 25.3°, PSL = −24.3dB. The visible region is delimited by the withe circle, wheras the blue colored areas indicate the sidelobe region.

of ϕ (denote the polar angle). For this case, in Fig.14 the optimized element layout, composed of Ne=105 active elements, is plotted. The method allows a saving of about 13.2% of the array elements with respect to the competing design [11] still keeping a very accurate pattern matching. In Fig.15 the broadside 3D-radiation pattern is plotted in the desired region of the (u, v) domain such that $u^2 + v^2 \leq [1 + sin(\theta_M)]^2$ with $\theta_M = 51°$. The u-cut and v-cut of the synthesized pattern are plotted in Fig.16. Fig. 17 plots the normalized array factor for a steering direction angle of $(\theta, \phi) = (51°, 0°)$. As it can be noticed, the proposed approach has capability to scan the beam, without the appearance of grating lobes in the whole visible range (i.e. $sin(\theta_M) = 0.7771$ and $U_{max} = 1.7771$).

The directivity of the maximally sparse linear array is 21.0262dB, whereas in the isophoric one (uniform weighting for all active elements) it is 21.8269dB, thus giving a ratio between the latter and the former directivity of 0.8dB (this confirms it is non-superdirective). The area bounded in our design is slightly smaller than $25\lambda^2$ [11], which is equal to $23.625\lambda^2$.

IV. CONCLUSION

A sequential convex optimization based approach for the synthesis of linear and planar sparse arrays generating focused beampattern is presented. The main advantages of the proposed approach can be summarised as follows. (a) For the considered benchmark problem, considerable improvements are obtained in terms of required radiation characteristics and the minimum number of required radiating elements. (b) The optimal solution can be more easily found since there is no parameter to be tuned (fixed parameter $\mu = 0.45$) contrary to stochastic optimization procedures in which the fine tuning of the numerous control parameters is definitely a difficulty. (c) The positions of the elements are fixed at predefined values, which makes the designed sparse array more realisable in practice. (d) The presented approach allowed a significant reduction of CPU time with respect to the other considered methods, thus the proposed design can be used for real-time applications. Furthermore, the maximally sparse array, able to radiate the steerable power pattern satisfying the provided specifications. The trend of the reduction in the number of array elements with respect to the steering intervals has been also investigated. The array imperfections are also considered in the optimization stage by using worst-case optimization technique. Finally, there is no restriction regarding the array geometry to be synthesized. Indeed, arbitrary arrays and any beam patterns (monopulse tracking applications, etc) can be handled.

REFERENCES

[1] A. Trucco, E. Omodei, and P. Repetto, "Synthesis of sparse planar arrays," *Electron. Lett.*, vol. 33, no. 22, pp. 1834–1835, 1997.
[2] A. Trucco, "Weighting and thinning wide-band arrays by simulated annealing," *Ultrasonics*, vol. 40, nos. 1–8, pp. 485–489, May 2002.
[3] O. Quevedo-Teruel and E. Rajo-Iglesias, "Ant colony optimization in thinned array synthesis with minimum sidelobe level," *IEEE Antennas Wireless Propag. Lett.*, vol. 5, pp. 349–352, 2006.
[4] R. Haupt, "Thinned arrays using genetic algorithms," *IEEE Trans. Antennas Propag.*, vol. 42, no. 7, pp. 993–999, Jul. 1994.
[5] J. W. Hooker and R. K. Arora, "Optimal thinning levels in linear arrays," *IEEE Antennas Wireless Propag. Lett.*, vol. 9, pp. 771–774, 2010.
[6] S. E. El-Khamy, A. S. Eltrass, and H. F. El-Sayed, "Design of thinned fractal antenna arrays for adaptive beam forming and sidelobe reduction," *IET Microw., Antennas Propag.*, vol. 12, no. 3, pp. 435–441, Feb. 2018.
[7] T. Isernia, F. Arespena, O. Bucci, M. D'urso, J. Gomez, and J. Rodriguez, "A hybrid approach for the optimal synthesis of pencil beams through array antennas," *IEEE Trans. Antennas Propag.*, vol. 52, no. 11, pp. 2912–2918, Nov. 2004.
[8] M. D'urso and T. Isernia, "Solving some array synthesis problems by means of an effective hybrid approach," *IEEE Trans. Antennas Propag.*, vol. 55, no. 3, pp. 750–759, Mar. 2007.
[9] S. E. Nai, W. Ser, Z. L. Yu, and H. Chen, "Beampattern synthesis for linear and planar arrays with antenna selection by convex optimization," *IEEE Trans. Antennas Propag.*, vol. 58, no. 12, pp. 3923–3930, Dec. 2010.
[10] M. D'urso, G. Prisco, and R. M. Tumolo, "Maximally sparse, steerable, and nonsuperdirective array antennas via convex optimizations," *IEEE Trans. Antennas Propag.*, vol. 64, no. 9, pp. 3840–3849, Sep. 2016.
[11] D. Pinchera, M. D. Migliore, and G. Panariello, "Synthesis of large sparse arrays using IDEA (inflating–deflating exploration algorithm)," *IEEE Trans. Antennas Propag.*, vol. 66, no. 9, pp. 4658–4668, Sep. 2018.

[12] S. E. El-Khamy, N. O. Korany, and M. A. Abdelhay, "Minimising number of perturbed elements in linear and planar adaptive arrays with broad nulls using compressed sensing approach," *IET Microw., Antennas Propag.*, vol. 13, no. 8, pp. 1134–1141, Jul. 2019.
[13] A. F. Morabito and P. Rocca, "Reducing the number of elements in phase–only reconfigurable arrays generating sum and difference patterns," *IEEE Antennas Wireless Propag. Lett.*, vol. 14, pp. 1338–1341, 2015.
[14] P. Rocca and A. F. Morabito, "Optimal synthesis of reconfigurable planar arrays with simplified architectures for monopulse radar applications," *IEEE Trans. Antennas Propag.*, vol. 63, no. 3, pp. 1048–1058, Mar. 2015.
[15] T. Zhang and W. Ser, "Robust beampattern synthesis for antenna arrays with mutual coupling effect," *IEEE Trans. Antennas Propag.*, vol. 59, no. 8, pp. 2889–2895, Aug. 2011.
[16] S. Boyd and L. Vandenberghe, *Convex Optimization*. Cambridge, U.K.: Cambridge Univ. Press, 2004.
[17] W. P. M. N. Keizer, "Element failure correction for a large monopulse phased array antenna with active amplitude weighting," *IEEE Trans. Antennas Propag.*, vol. 55, no. 8, pp. 2211–2218, Aug. 2007.
[18] W. P. M. N. Keizer, "Fast Low–Sidelobe synthesis for large planar array antennas utilizing successive fast Fourier transforms of the array factor," *IEEE Trans. Antennas Propag.*, vol. 55, no. 3, pp. 715–722, Mar. 2007.
[19] W. Keizer, "Large planar array thinning using iterative FFT techniques," *IEEE Trans. Antennas Propag.*, vol. 57, no. 10, pp. 3359–3362, Oct. 2009.
[20] W. P. M. N. Keizer, "Low-sidelobe pattern synthesis using iterative Fourier techniques coded in MATLAB," *IEEE Antennas Propag. Mag.*, vol. 51, no. 2, pp. 137–150, Apr. 2009.
[21] W. P. M. N. Keizer, "Low sidelobe phased array pattern synthesis with compensation for errors due to quantized tapering," *IEEE Trans. Antennas Propag.*, vol. 59, no. 12, pp. 4520–4524, Dec. 2011.
[22] W. P. M. N. Keizer, "Amplitude–only low sidelobe synthesis for large thinned circular array antennas," *IEEE Trans. Antennas Propag.*, vol. 60, no. 2, pp. 1157–1161, Feb. 2012.
[23] X.-K. Wang, Y.-C. Jiao, and Y.-Y. Tan, "Synthesis of large thinned planar arrays using a modified iterative Fourier technique," *IEEE Trans. Antennas Propag.*, vol. 62, no. 4, pp. 1564–1571, Apr. 2014.
[24] W. P. M. N. Keizer, "Synthesis of thinned planar circular and square arrays using density tapering," *IEEE Trans. Antennas Propag.*, vol. 62, no. 4, pp. 1555–1563, Apr. 2014.
[25] B. Fuchs, A. Skrivervik, and J. R. Mosig, "Shaped beam synthesis of arrays via sequential convex optimizations," *IEEE Antennas Wireless Propag. Lett.*, vol. 12, pp. 1049–1052, 2013.
[26] G. Prisco and M. D'urso, "Maximally sparse arrays via sequential convex optimizations," *IEEE Antennas Wireless Propag. Lett.*, vol. 11, pp. 192–195, 2012.
[27] B. Fuchs, "Synthesis of sparse arrays with focused or shaped beampattern via sequential convex optimizations," *IEEE Trans. Antennas Propag.*, vol. 60, no. 7, pp. 3499–3503, Jul. 2012.
[28] J. Liu, Z. Zhao, K. Yang, and Q. H. Liu, "A hybrid optimization for pattern synthesis of large antenna arrays," *Prog. Electromagn. Res.*, vol. 145, pp. 81–91, 2014, doi: 10.2528/PIER13121606.
[29] R. J. Mailloux, "Array failure correction with a digitally beamformed array," *IEEE Trans. Antennas Propag.*, vol. 44, no. 12, pp. 1543–1550, Dec. 1996.
[30] B.-K. Yeo and Y. Lu, "Array failure correction with a genetic algorithm," *IEEE Trans. Antennas Propag.*, vol. 47, no. 5, pp. 823–828, May 1999.
[31] *CVX: MATLAB Software for Disciplined Convex Programming*. Accessed: Sep. 7, 2018. [Online]. Available: http://cvxr.com/cvx/
[32] K. Yang, Z. Zhao, and Q. H. Liu, "Fast pencil beam pattern synthesis of large unequally spaced antenna arrays," *IEEE Trans. Antennas Propag.*, vol. 61, no. 2, pp. 627–634, Feb. 2013.
[33] K. Yang, Z. Zhao, and Y. Liu, "Synthesis of sparse planar arrays with matrix pencil method," in *Proc. Int. Conf. Comput. Problem-Solving (ICCP)*, Oct. 2011.